State-of-the-RNArt: benchmarking current methods for RNA 3D structure prediction

Clément Bernard[1,2], Guillaume Postic[1], Sahar Ghannay[2], and Fariza Tahi[1]

[1]Université Paris Saclay, Univ Evry, IBISC, 91020, Evry-Courcouronnes, France

[2]LISN - CNRS/Université Paris-Saclay, France, 91400, Orsay, France

RNAs are essential molecules involved in numerous biological functions. Understanding RNA functions requires the knowledge of their 3D structures. Computational methods have been developed for over two decades to predict the 3D conformations from RNA sequences. These computational methods have been widely used and are usually categorised as either *ab initio* or template-based. The performances remain to be improved. Recently, the rise of deep learning has changed the sight of novel approaches. Deep learning methods are promising, but the adaptation to RNA 3D structure prediction remains at stake. In this work, we give a brief review of the *ab initio*, template-based and novel deep learning approaches. We highlight the different available tools and provide a benchmark on nine approaches using the RNA-Puzzles dataset. We provide an online dashboard that shows the predictions made by benchmarked models, freely available on the EvryRNA platform: https://evryrna.ibisc.univ-evry.fr.

RNA 3D structure | *Ab initio* | Template-based | Deep learning

Correspondence: *fariza.tahi@univ-evry.fr*

Introduction

Ribonucleic acids (RNAs) are macromolecules that play diverse biological roles in living organisms. RNAs are involved in numerous physiological processes, such as protein synthesis, RNA splicing, or transcription regulation, as well as in various human diseases. RNAs also have the potential to be used as therapeutic agents for different purposes, like cancer (1). Understanding RNA functions is a challenging task that has been studied for decades.

The biological function of RNA is, like protein, determined by the 3D conformation of the molecule. This folding can be determined by experimental methods like X-ray crystallography, NMR or, more recently, cryo-EM (2). Nonetheless, these methods are costly both in time and resources. On the other hand, sequencing methods (like next-generation sequencing (3)) have progressed and a large number of sequences has become available without any structural data. As a result, there is a huge gap between the known RNA sequences compared to the solved 3D structures. Up to December 2023, there are 7,296 solved RNA structures in the PDB (4) compared to 2,924,924 RNA sequences in Rfam (5). Only 136 out of 4,170 RNA families have at least one known structure. Therefore, computational methods have been developed for the past decades to compute RNA 3D structure from the sequence. Two main approaches have emerged: the *ab initio* and the template-based. While the first uses molecular dynamics and force fields, the latter relies on a database of known structures. None of these approaches predicts RNA structure perfectly and methods still emerge.

During the CASP (6) competition, AlphaFold (7, 8) from DeepMind recently predicted protein 3D structures. The team used deep learning techniques to predict the atomic positions of each amino acid of the sequence with high precision. The adaptation of this architecture can not be applied to RNA due to the protein and RNA intrinsic biological differences. Indeed, the sequences are different between RNA and proteins in terms of individual elements (amino-acid compared to nucleotides), diversity of sequence range, the number of available structure data and the stability of the folding (a given sequence of protein can fold into one stable conformation compared to multiple conformations for RNA). Nevertheless, deep learning methods have emerged to predict RNA structures from sequences with relative success. Predicting RNA tertiary structures from sequence remains an open problem to be solved.

Works have been done to review the state-of-the-art existing methods. A recent study (9) describes up-to-date models while highlighting the need to use probing data. Another review (10) also describes past methods and points out the detailed types of inputs that can be integrated into developed models. On the other hand, a review (11) describes only the *ab initio* methods with the force fields used for each method. A final recent review (12) discusses recent advances in terms of RNA but is not specific to the 3D structures. It sheds light on the machine learning advancements in the RNA field.

In this paper, we aim to give the reader a comprehensive overview of the RNA 3D structure prediction. Through a detailed description of *ab initio*, template-based and deep learning approaches, we detail the available tools and benchmark them on a dataset to compare their performances. The results are easily reproducible and an interface with the predicted 3D structures is provided and freely available on the EvryRNA platform: https://evryrna.ibisc.univ-evry.fr. The user can interact with the dashboard to select the challenge to visualize and look at the different predictions computed for the bench-

mark.

The paper is organised as follows: we first present RNA 3D structure specificities at stake for its prediction. We then provide an overview of the main predictive methods developed through decades for predicting RNA 3D structure. We give a broad overview of the field and include state-of-the-art deep learning approaches, with published or preprint works. Finally, we benchmark the available models on a dataset to provide an overview of current performances.

Methods

Computational methods aim to predict the atomistic positions and interactions in the RNA molecule. They tend to follow the same steps: sampling the conformational space (creation of a set of candidate structures) and discrimination of the candidates. The final structure is usually chosen with either the lowest energy or the center of a cluster of lowest energy structures. Methods can be classified as *ab initio*, template-based or deep learning-based. *Ab initio* methods integrate the physics of the system, while template-based methods are based on constructing a database that maps sequences to known motifs. Deep learning approaches use available data to create a neural network architecture that predicts RNA 3D structures from sequence or MSA (Multiple Sequence Alignment).

We present in the following a description of the state-of-the-art methods for RNA 3D structure prediction. The methods are organised by approach type (*ab initio*, template-based and deep learning) and chronologically. The implementation availability in terms of web server and standalone code is provided for each method. A summary of the state-of-the-art tools, including information on the implementation, is given in Table S1 of the Supplementary file.

Ab initio methods

Ab initio (or prediction-based) methods tend to simulate the physics of the system. It also captures the folding dynamics, such as energy landscapes. RNA molecules are represented at the atom level, and forces are applied to simulate real environment conditions. To explore the conformation space, sampling algorithms are used, like Monte Carlo (MC) (13) or molecular dynamics sampling (14). As the simulation can be time-consuming, a key parameter of *ab initio* methods is the granularity of the nucleotide representation. It is defined as the number of beads per nucleotide, where atoms are omitted to be replaced by representative ones. A bead refers to the number of atoms per nucleotide, which defines the granularity of the method. NAST (15), for instance, uses one atom per nucleotide, while other methods like iFoldRNA (16), OxRNA (17), HIRE-RNA (18), SimRNA (19), IsRNA1 (20), IsRNA2 (21) and RNAJP (22) tend to have more atoms per nucleotide. Other methods use different granularity like helix as a base with Ernwin (23) or BARNACLE (24) with a bayesian model. The force field used in the simulation must be adapted to the new nucleotide representation. The simulation might be more realistic but more time-consuming if all nucleotide atoms are represented. It could also miss sampling space where there are low-energy structures. On the other hand, if the number of beads is low for the representation of nucleotides, the simulation might be faster. Reducing the number of atoms would also reduce the system's degrees of freedom and thus simplify the sampling phase, but would result in a less accurate folding. Even more, it might fail to represent stacking and base-pairing interactions. On top of this representation, a full atom reconstruction is needed to map the bead to actual atoms of nucleotides. Therefore, this trade-off is a key component discussed and used through *ab initio* works.

iFoldRNA (16) is a three-bead per nucleotide method with discrete molecular dynamics to simulate the RNA folding process. Another version of iFoldRNA, called iFoldRNA v2 (25), adds clustering on RMSD after simulation to reconstruct the center of founded clusters. Each bead represents a phosphate, sugar or nucleobase. The force field incorporates angle interactions, base pairing, base stacking, or hydrophobic interactions.

A web server is provided, but not the source code. The web server requires having an account. When connected, a user can request structures with a sequence and, optionally, a 2D structure. The computation time is high: a sequence with less than 100 nucleotides takes more than one day to be processed.

NAST (15) models at the one-point-per-residue resolution but considers the geometrical constraints from ribosome structures before discriminating the obtained structures with root-mean-square deviation. It utilizes knowledge-based statistical potential to guide the simulation and cluster-generated structures. The bead is located at the $C3'$ atom.

No web server is provided; the source code is available and written in Python 2.

BARNACLE (24) uses another method, a Bayesian parametrized model using the seven angles characterizing a nucleotide with a hidden Markov chain process. It models marginal distributions for the dihedral angles using a mixture of probability distributions. It links the dependencies between angles with a Markov chain of hidden states. It helps reduce input representation while capturing the length distribution of helical regions.

No web server is provided, but the source code is available. We tried to run the code, but we got errors. We also tried to convert the Python 2 code to Python 3 without success.

OxRNA (17) is a 5-bead coarse-grained approach that uses both virtual move Monte Carlo (VCMC) and umbrella sampling (26) to sample the conformational space. It manages to characterize the thermodynamics of RNA molecules. The potential energy of the model splits terms that are non-nearest-neighbour pairs of nucleotide and neighbours. It also incorporates temperature dependence, as the coarse-grained interaction is assumed to be free energy rather than potential

energy.

A web server and source code are available. Nonetheless, the source code details the web server. The required inputs for the local or web servers are of a specific format, with configuration and topology files. Therefore, it is not straightforward to properly convert a sequence to server inputs.

Ernwin (23) uses Markov chain Monte Carlo (MCMC) with a helix-based model that maps the helices to cylinders and loops to close edges connected to a helix. The force field used five energy terms like steric clash energy or knowledge-based potential of mean force.

A web server and a source code are available. The web server only returns coarse-grained molecules. There is still, up-to-date, no full-atom reconstruction included.

HiRE-RNA (18) shows that noncanonical and multiple base interactions are necessary to capture the full physical behaviour of complex RNAs, with a six-bead nucleotide method. It uses a model with geometric parameters determined from 200 structures. The potential integrates stacking and base-pairing terms that consider base orientations. The Replica-Exchange Molecular Dynamics (REMD) simulations are used for sample strategies.

There is no web server nor source code available.

SimRNA (19) uses Monte Carlo steps with a five-bead nucleotide approach guided by an energy that considers local and non-local terms. The local term includes bond length or angle interactions, while non-local terms consider base-to-backbone interactions. The sampling procedure is the asymmetric Metropolis algorithm (27). The predicted structures are based on clustering methods of lower energies.

Web server and standalone server are available. The code is well-documented and can be used easily. The web server is hardly usable as it can only have three jobs at a time. Multiple days are required to process a prediction, preventing automation and easy access to the model. When running locally with default parameters, the outputs were always the same and did not relate to any RNA tertiary structure.

IsRNA, **IsRNA1** (20) and **IsRNA2** (21) are based on a coarse-grained method with five-bead per nucleotide to predict noncanonical base pairs. The energy used includes bond length, bond angle bending and torsion angle energies. It also combines covalent energy functions for base-pairing interactions. It adds non-local terms like base-base, base-backbone and backbone-backbone interactions. In the IsRNA1 model, the canonical base-pairing adds interaction distances to consider bond strength compared to IsRNA (28). IsRNA2 better integrates noncanonical base pairing interactions in large RNAs compared to IsRNA1.

A web server is available for IsRNA1, while the source code can only be downloaded with an account. The installation requires multiple libraries that also require having an account on other websites. The web server takes multiple hours for predictions around hundreds of nucleotides.

RNAJP (22) uses a coarse-grained approach at both atom and helix levels. It represents a nucleotide with five beads to describe the Watson-Crick, Hoogsten and sugar edges in bases. The force field used is a sum of 12 energy terms considering bonded interactions in length, bond and torsion angles, as well as base pairing and base stacking interactions. The energy integrated uses terms for the manipulation of helices and loops.

No web server is available; the source code can only be downloaded with an account. We had errors with the *bp_stk_paras* folder, where capitalization variations were missing. We managed to get the program running by modifying this folder.

Using physics-based modelling, coarse-grained approaches can predict RNA tertiary structures from raw sequences. The energy-based scoring function helps discriminate or guide predicted structures. Final predictions are usually either the lowest energy molecules or centroid of clusters. Current coarse-grained approaches fail to consider the formation of non-canonical pairs and, even more, the base side of interactions. The size of the considered RNA limits those methods: the longer the sequence, the more time-consuming the simulation is. The increase in the sequence length is not linear with the simulation time: the number of conformational states grows exponentially with the sequence. Having an efficient sampling method is a challenging task and the key to efficient *ab initio* methods. The final limitation of those methods is the discriminator function, which is usually energy-based. An inaccurate energy function could result in a non-native predicted structure and bias the sampling method, which often guides the sampling procedure.

Template-based methods

Template-based (or fragment-assembly) approaches rely on the fact that molecules that have evolution similitude adopt similar structures. A template molecule can be used as a structural basis, where other mutated sequences tend to retain similar and global conformations. A database of known RNA structures is used as a reference. Those structures have a mapping between their sequence and motif/structure/fragment. The size of the fragments considered is a key parameter for the efficiency and accuracy of the method. It can be at the nucleotide level or at the secondary structure elements (SSEs) level, for instance. Methods like RNABuilder (29), ModeRNA (30) use one nucleotide per fragment, while FARNA/FARFAR (31) and FARFAR 2 (32) use three nucleotides per fragment. MC-Sym (33), RNAComposer (34), Vfold (35), VfoldLA (36), 3dRNA (37), Vfold Pipeline (38) and FebRNA (39) consider as base representation SSEs. The predicted structure can be refined to prevent clashes with energy minimization.

FARNA/FARFAR (31) is one of the first template-based methods to predict RNA 3D structures. It is inspired by

Rosetta low-resolution protein structure prediction method (40). It uses an energy function of six terms relying on physics-based constraints, a metropolis criterion for fragment assembly using torsion angles replaced at each Monte Carlo step. While energy is computed atomistically with FARFAR, FARNA uses a simplified coarse-grained potential. Both energies can form non-canonical pairs but are limited by size and cannot predict large molecules. It uses short segments as blocks (three-nucleotide segments) and thus needs numerous MC samplings to find a stable structure. FARFAR 2 (32) was proposed to increase the accuracy and speed. It also adds a clustering method to discriminate the most common structures.

There is a web server for FARFAR and FARFAR 2, but no source code is available. The prediction time is quite high, with multiple days for a single prediction.

MC-Sym (33) uses the SSEs, with nucleotide cycle modulus as blocks. It inputs both raw sequence and 2D structures from MC-Fold (33) method to minimize the physics-based force field. It relies on a representation of nucleotide relationships named nucleotide cyclic motif (NCM), incorporating more context-dependent information. This representation is used to infer a scoring function used for both secondary and tertiary structure prediction. A database with lone-pair loops and double-stranded NCMs is used in the pipeline and in the scoring function.

While being well documented for using a web server, the source code is unavailable. The web server is user-friendly, and there is almost no waiting time for a job to run. It requires only secondary structures from MC-Fold to predict 3D structures.

RNABuilder (29) uses multi-resolution modelling (MRM) and multibody dynamics simulation. It is based on a target-template alignment that assigns correspondences between residues and spatial constraints. It is described to predict *Azoarcus* group I intron and can be extended to other structured RNAs. It uses features from SimTK. It combines secondary and tertiary base pairing contacts in the force field. It can also solve structures with small connecting regions without a template.

No web server is available but a source code is available, well-documented and usable.

ModeRNA (30) searches for fragments in a database to replace the mutated structure before using energy minimization to refine the final structure. It uses atomic coordinates of the template and prevents backbone discontinuities by adding short fragments of other structures. It provides different strategies to build RNA structures that can be modified easily.

A web server and a code are provided. We did not try the web server's predictions because it required 3D structures as inputs.

Vfold3D (41) constructs 3D structures from fragment databases. It uses the lowest free energy secondary structures converted to known fragments. The reconstruction of fragments is coarse-grained before being converted to all-atom. The final refinement of the structures uses AMBER energy minimization (42, 43). **VfoldLA** (36) uses a template database with single-stranded loops or junctions. Instead of searching for whole motifs, its granularity is finer and allows smaller blocks to be integrated. It helps prevent the limit of Vfold3D, which uses whole motifs limited by the number of available RNA data. Integration of the previous methods has been done in **Vfold-Pipeline** (38). Given a sequence in input, the pipeline uses Vfold2D to predict the secondary structure and then uses either Vfold3D or VfoldLA for the final 3D structure prediction.

A web server is available for either Vfold3D, VfoldLA and Vfold-Pipeline. The source code is also available and usable.

RNAComposer (34) creates a database (named FRABASE) with fragment mapping 2D elements to 3D motifs before using refinement. The SSEs are used as minimum blocks to assemble the different fragments. The method uses the Kabsch algorithm (44) to assemble the 3D structure elements. The refinement of the structure concatenates two energy minimization methods: torsion angles energy (using CYANA (45)) and atom coordinate with CHARMM (46).

There is a web server accessible, but no source code is provided.

3dRNA (37, 47) uses a fragment assembly approach guided by their scoring function 3dRNAScore (48), where the SSEs considered are improved by more base pairs from connected stems. It uses SSEs as blocks and predicted structures come from a clustering approach using 3dRNAScore as criteria. An improvement of the 3D template library is proposed in 3dRNA (49) by an increase of about ten times the number of templates.

A web server is provided, and the source code is available only after login. It is required to have other software installed to run the standalone code.

FebRNA (39) creates a 3D fragment ensemble and identifies the 3D coarse-grained structure using cgRNASP (50) score, with three-bead per nucleotide. It performs all-atom reconstruction followed by refinement. The building of fragments is executed with secondary structure tree (SST) (51), where each stem is considered a node of a tree structure. It then builds a 3D structure through sequential superposition between coarse-grained atoms of a loop and stem according to the SST order.

No web server is accessible, but the source code is available and well-documented. Nevertheless, we did not manage to run the code because we had errors.

Template-based methods allow the prediction of RNA 3D structures with the help of available data. They create a database mapping sequence to fragments (or motifs) before

assembling it to refine final structures. However, the number of experimental RNA structures is a bottleneck for the good accuracy of the models. Templates like SSEs tend to be inaccurate or missing in the constituted database, preventing good predictions of structures. They also fail to generalize to unseen structures. As many RNA families are not yet discovered, such approaches would probably fail to predict new families.

Deep learning approaches

In the CASP competition, an end-to-end approach has been introduced and overperformed all previous works for predicting protein 3D structure: AlphaFold (7, 8). It has changed the structural biology field and raised the interest of researchers. Recent works have been done to predict RNA 2D structures (52, 53), as the available data is much higher than solved 3D structures. Other deep learning works try to predict energy function (54, 55), while others infer torsion angles from the sequence (56). Such angles can nevertheless be used to help the prediction of 3D structures. Preprint works have been released like DeepFoldRNA (57), RhoFold (58), RoseTTAFoldNA (59), and NuFold (60) to predict 3D structures with attention-based (61) methods. Three deep learning approaches, epRNA (62), DRfold (63) and trRosettaRNA (64), have recently been published. As the advancement in the field is moving fast, we describe both preprint and published works in the following.

DeepFoldRNA (57) is a preprint work that predicts RNA structures from sequence alone by coupling deep self-attention neural networks with gradient-based folding simulations. It predicts distance and orientation maps, as well as torsion angles, with transformer-like blocks. It uses MSA and 2D structure as inputs. A BERT-like (65) loss was also implemented to make the model more robust. To get around the lack of data, a self-distillation approach used sequences from bp-RNA-1m (66). To convert the neural network outputs to 3D structures, it uses L-BFGS (67) folding simulations with energy defined by the weighted sum of the negative log-likelihood of the binned probability predictions.

A web server and a source code are provided. We tried to predict sequences from the web servers but never received the results.

RhoFold (58) is a preprint work with an end-to-end differentiable approach for predicting RNA 3D structures. The model's input is the MSA, and features are extracted with a pre-trained model RNA-FM (68) trained over more than 23 million sequences. It gives an MSA co-evolution matrix and pairwise residue features. A module called E2EFormer with gated attention layers is applied to predict the main frame (C'_4, C'_1, N_1/N_9) in the backbone and four torsion angles ($\alpha, \beta, \gamma, \omega$). An IPA (invariant point attention) is used in modelling 3D positions. It predicts each frame's rotation and translation matrices based on the sequence and pair representation from the E2Eformer module. Given the predicted frames and angles, the structure module can generate the full-atom coordinates of an RNA without simulation. It also uses self-distillation with bp-RNA-1m (66) and combines the training process with a loss that takes into account 1D (sequence masking), 2D and 3D (Frame Aligned Point Error (FAPE)) elements.

A web server and a source code are provided. The web server is easily usable, while the standalone code requires more than 500 GB of space to download the database, even for inference.

RoseTTAFoldNA (59) is a preprint work with an end-to-end deep learning approach that predicts 3D structure for RNA molecules and protein-DNA and protein-RNA complexes. It incorporates three representations of molecules: sequence (1D) with MSA representation, residue-pair distances (2D) and cartesian coordinates (3D). The 3D representation uses the position and orientation of phosphate, as well as torsion angles. The model can take as input protein, DNA and RNA. It was trained on five types of structures: protein structures, AlphaFold2 predictions, protein complexes, protein/NA complexes and RNA structures. Two losses were used: one for the training process and the other for the fine-tuning stage. The first loss is a weighted sum of distogram loss, structure loss (averaged backbone FAPE loss (8) over structure layers of the model), torsion prediction loss and pLDDT loss. The second loss incorporates energy terms to ensure model feasibility.

A source code is provided, but no web server exists. The source code requires more than 500Gb of free space to download sequence and structure databases.

trRosettaRNA (64) is a published work inspired by AlphaFold2 (8) and trRosetta (69–71). It uses MSA and secondary structure (using SPOT-RNA (72)) as inputs. The network architecture is inspired by AlphaFold2 Evoformer block and thus uses transformer networks. The full atom reconstruction uses energy minimization with restraints from predicted geometries weighted by parameters optimized from random RNA from the training set. The model is trained on PDB data with sequences that have homologs. They use bpRNA (66) from Rfam (5) to use self-distillation to increase the available data. Distillation is regulated with a Kullback-Leibler divergence.

A web server is available, but no standalone code.

epRNA (62) is a published work with an Euclidean parametrization-based neural network that predicts RNA tertiary structure from sequence only. It is trained to predict a distance matrix that is then validated with Hoffmann and Noé (73) algorithm and added to the loss. The network uses convolutional networks and uses one hot encoding as input. It uses RNA from the PDB and splits it into training and test sets (60% for training and 40% for testing). The method achieves E(3) invariance (rotations, translations and reflections) but does not achieve SE(3) invariance. It means that the mirror image of a chiral molecule is chemically distinct, but this distinction is not made in the network.

A source code is available, but no web server. The code is easy to use, and the installation process is straightforward. There is no need to install huge datasets to perform predictions.

NuFold (60) is a preprint work with a direct adaptation of AlphaFold2 work for RNAs. It considers the base frame with four atoms: $O4'$, $C1'$, "C4' and either $N1$ (for C and U) or $N9$ (for G and A). It also adds heads to predict the distance between $C4'$ and P, and the dihedral angle between residue pairs. It uses as inputs MSA and secondary structure predicted by IPknot (74). The NuFold network comprises two key components: the EvoFormer block and the structure model. The EvoFormer part is a transformer model that embeds information into single and pair representations. The structure model converts the embedding into 3D structures. It is recycled three times to increase the accuracy of predictions. The network outputs are the translation and rotation of the four base frames and torsion angles. The torsion angles help the reconstruction of full-atom representation.

No web server is available, and no code yet. It is said that the code will be available after a clean-up by the authors.

DRfold (63) is a published work with an end-to-end transformer-based approach that takes as input RNA sequence and secondary structure. It uses a three-bead representation for a nucleotide. It converts the inputs into sequence and pair representations before feeding them to transformer blocks. A structure module outputs frames converted to FAPE potential (frame aligned point error), while a geometry module predicts rotation and translation property converted to geometry potentials. These predicted frame vectors and geometry restraints are aggregated to a potential for structure reconstruction. The final step includes all-atom reconstruction and refinement using Arena (75) and OpenMM (76).

No web server is provided, but a source code is available. It requires the download of numerous libraries.

Deep learning methods are promising and have good performances on testing datasets. Nonetheless, deep learning models need a huge amount of data, which is unavailable for RNA 3D structures. To avoid this bottleneck, methods use self-distillation. They also mainly input MSA representation like AlphaFold. MSA remains a limitation as the number of known RNA families is restricted. The overall quality of the predicted structures remains to be validated with new data from unseen families.

Results

In this section, we detail the results of the different approaches on a test set of RNA structures. To have a fair comparison between existing models, we benchmark them on a unique test set widely used in the community, RNA-Puzzles (77). We predict structures from usable models and compare them using standard metrics described in previous work (78). These results aim to provide a state-of-the-art overview of the performance differences from raw predictions, available for every user with the available web servers.

Benchmarked tools

As discussed in the previous section and summarized in Table S1 of Supplementary file, some of the state-of-the-art methods do not have a web server or a standalone code available. It is the case of Hire-RNA (18) and NuFold (60). Among the remaining tools, unfortunately, many are hard to use or not working. Among the available standalone codes, we only manage to run RNAJP (22), while the other tools like DeepFoldRNA (57), FebRNA (39) or RoseTTFoldNA (59) require the download of databases. Those databases could have more than 500Gb and thus be hardly usable for users. Other tools like Ernwin (23) or epRNA (62) only return coarse-grained structure and thus increase the use complexity. Among the web servers usable, ModeRNA (30) needs as input an initial 3D structure, which we did not have for the benchmark. OxRNA (17) requires a specific input format, which makes it hard for the user to use. SimRNA (19) and FARFAR 2 (32) have web servers, but we considered the computation time as too long to include it. DeepFoldRNA (57) and Drfold (63) have web servers where we did not get the structures after making the request. We made some of the predictions for iFoldRNA (16), but we found the server very hard to connect to and thus failed to make all the predictions.

As a benchmark, we thus considered the remaining nine methods described in Table 1. We used RNA-tools (79) to clean the predicted structures and to normalize them. This software enables the operation of RNA structures and allows their standardisation to help better evaluate them. All models were used with their web servers except for RNAJP, which was used locally. We set a computation limit for RNAJP computation.

Not all tools could predict directly from the sequences. We decided, when needed, to use the secondary structure predicted by MXFold 2 (80), a recent deep learning-based tool giving good prediction results. The choice of MXFold 2 was arbitrary but should be consistent between the models to have a fair comparison. For MC-Sym, it is required a secondary structure from MC-Fold (33).

Model	Server inputs	Method
MC-Sym (33)	Seq+2D	Template-based
Vfold3D (41)	Seq+2D	Template-based
RNAComposer (34)	Seq+2D	Template-based
3dRNA (37)	Seq+2D	Template-based
IsRNA1 (20)	Seq+2D	*Ab initio*
RhoFold (58)	Seq	Deep Learning
trRosettaRNA (64)	Seq	Deep Learning
Vfold-Pipeline (38)	Seq+2D	Template-based
RNAJP (22)	Seq+2D	*Ab initio*

Table 1. Benchmark models as well as server inputs associated. Seq refers to the raw sequence, and 2D for the secondary structure. The inputs correspond to the required inputs from the web server; they may not correspond to what the model uses. For instance, IsRNA1 require the raw sequence and secondary structure, but the real input for the simulation is the predicted structure from IsRNA (28) and the secondary structure.

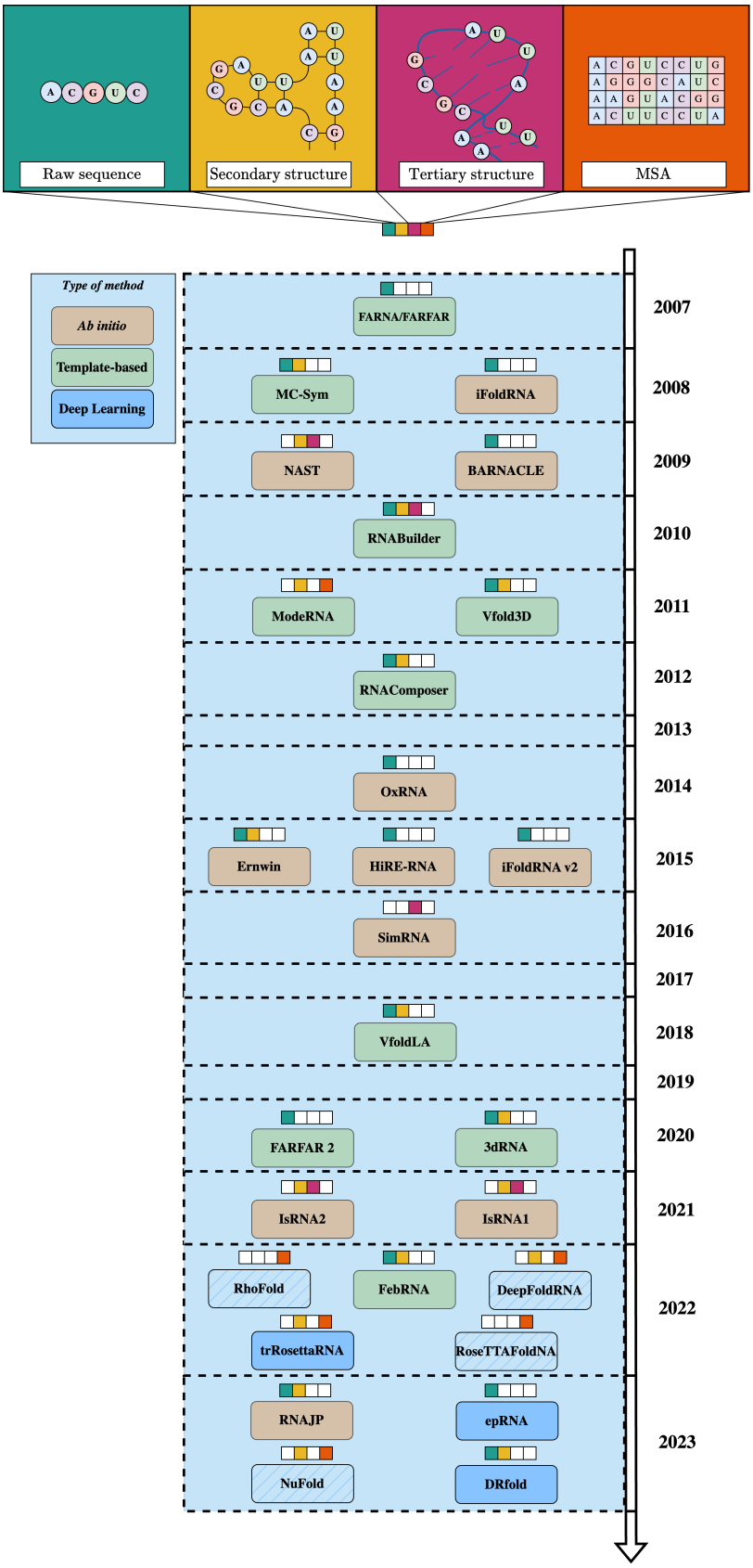

Figure 1. State-of-the-art of the main works for predicting RNA 3D structures. The different inputs are either raw sequence, secondary structure, tertiary structure or multiple sequence alignment (MSA). Hatched methods are preprint works.

Test Set

As an adaptation of the CASP competition, the community created RNA-Puzzles (77) in 2011. It is used as an RNA test set to assess the generalization property of models. The RNA molecules proposed through the years as a challenge are solved structures that have challenging properties: double-stranded structures, ribozymes, riboswitches and more. We decided to use this dataset as a benchmark. The dataset contains both single-stranded and multi-stranded RNAs, whereas not all models can predict RNA complexes (multi-stranded RNAs). We decided only to consider single-stranded RNAs for a fair comparison between models. It represents 22 RNAs with a sequence between 27 and 188 nucleotides. More details about the considered RNAs, as well as their families, are described in Table S2 of the Supplementary file.

A collaboration between RNA-Puzzles and CASP teams led to the CASP 15 (81) competition. 12 RNA targets were proposed, and around 40 groups tried to predict the RNA structures. The groups could work on predicting these 12 specific targets, which may have required some tuning to perform better. Therefore, we tried to predict the targets with nine models, but it led to non-realistic predictions. Most models did not predict RNA targets because the RNA sequences were too long. The RNA targets are complex and require more tuning to adjust model prediction. As we did not get a lot of predictions, we did not include results on CASP-RNA.

Evaluation metrics

To compare the quality of predictions, we used the Root-Mean-Square-Deviation (RMSD), which is very sensitive to local differences. The INF (82) metric tries to incorporate RNA key interactions to evaluate RNA 3D structures better. Another tentative to incorporate RNA specificities is the ϵRMSD (83). We also considered the TM-score (84, 85) and lDDT (86), which are, respectively, the normalisation of atom deviation metric and interatomic differences, both inspired by protein evaluation metrics. The P-VALUE (87) assesses if a prediction is better than a random one. RMSD, ϵRMSD and P-VALUE have good results when the values are low, whereas high values are better for INF, lDDT and TM-score. All these metrics were considered thanks to RNAdvisor (78), a benchmarking tool that helps the automation of RNA 3D structures evaluation. Mean values for each model and each metric are available in Table S3 of the Supplementary file.

Benchmark results

We compute the different metrics for predictions of template-based, *ab initio* and deep learning models. The distribution of each metric for each model is shown in Figure 2. It shows the outperformance of deep learning models compared to *ab initio* and template-based methods for almost every metric except for INF. The base interactions seem better reproduced for Vfold-Pipeline than other methods (higher distribution of INF). Deep learning approaches give an overall good shape (low RMSD, ϵRMSD, P-VALUE, lDDT and TM-score), but do not output all the key RNA interactions. *Ab initio* and template-based methods have almost the same distribution in terms of TM-score and ϵRMSD. Vfold-pipeline is slightly better for every metric compared to other *ab initio* and template-based approaches. Very low values of lDDT for MC-Sym, Vfold3D and RNAJP can be explained as computing errors as other metrics do not show the same outlier values in the distribution. The distributions for the complementary metrics are available in Figure S1 of the Supplementary file.

Detailed results of each model for each RNA are available in Figure 3. Missing values can be due to either a failure in the computation or in the prediction of the structures. For instance, the RMSD, ϵRMSD and P-VALUE have missing values for RNAJP for the puzzles rp32 and rp11, which is due to computation issues. MC-Sym, on the contrary, failed to predict challenges like rp21, rp34, rp12, rp06, rp07 and rp05. The figure highlights the good performances of trRosettaRNA for all the metrics. RhoFold also has good performances, especially for puzzle 34 (PDB ID: 7V9E). We observe high P-VALUE for some RNAs for RNAJP, 3dRNA, RNAComposer, Vfold-Pipeline, Vfold3D and MC-Sym. It means that some predictions can be close to random ones, whereas deep learning models are more confident and have almost never a high P-VALUE. The completed metrics are available in Figure S2 of the Supplementary file.

We arbitrarily selected a structure from the RNA-Puzzles challenge to observe the different predictions of the models. This molecule is puzzle 3, a Riboswitch (PDB ID: 3OWZ). The predicted structures from the different models with the native structure are shown in Figure 4. We did an alignment to show them on the same scale using the matching tool of Chimera (88). Vfold3D and Vfold-Pipeline have different predictions, meaning that Vfold-Pipeline has used VfoldLA for the 3D structure prediction. The model that seems to superimpose the reference well is the trRosettaRNA, with an RMSD of 2.38. The exact metric for each model for this RNA is shown in Table S4 of the Supplementary file. We observe good visual folding for the deep learning models and Vfold-pipeline. On the other hand, RNAJP and RNAComposer predictions do not seem to fit well with the native shape.

Computation time

We summarized the rough inference computation time to predict RNA 3D structures for each model in Table 2. We report the computation time for the RNA with the shortest and the most extended sequence. Vfold3D and Vfold-Pipeline are almost the same models. The only difference is the use of VfoldLA when Vfold3D does not provide predictions in Vfold-Pipeline. We observe that the *ab initio* methods have a computation time higher than the template-based and deep learning methods. This is due to the simulation processes that require a high number of computation steps. The template-based methods almost always return a structure with less than 2 hours of computation (including the queue in the web servers). On the other hand, deep learning methods tend to be very fast for inference. RhoFold predicts with high throughput, and what is the most time-consuming is the relaxation of

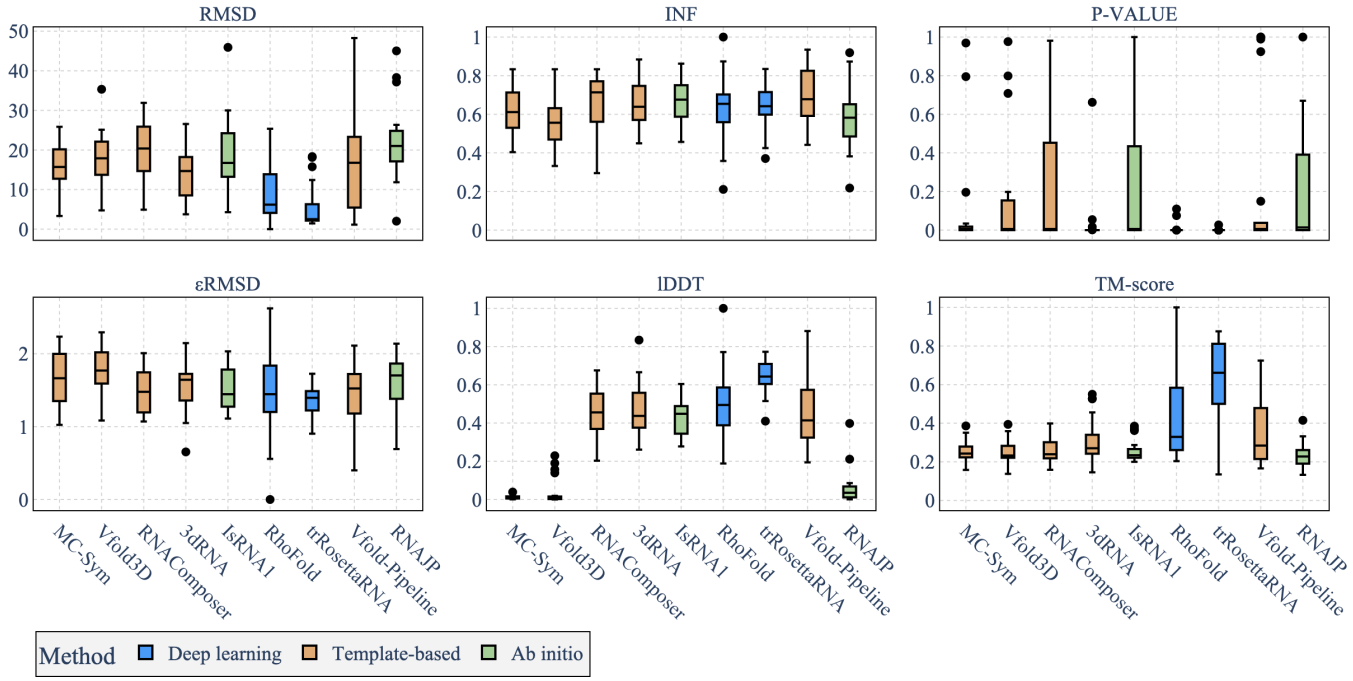

Figure 2. Results of a benchmark on single-stranded RNAs using RNA-Puzzles for the different models for RMSD, INF, P-VALUE, ϵRMSD, lDDT and TM-score metrics. Methods are sorted by release date. P-VALUE, RMSD and ϵRMSD are decreasing (the lower, the better) while TM-score, lDDT and INF are ascending and range between 0 and 1.

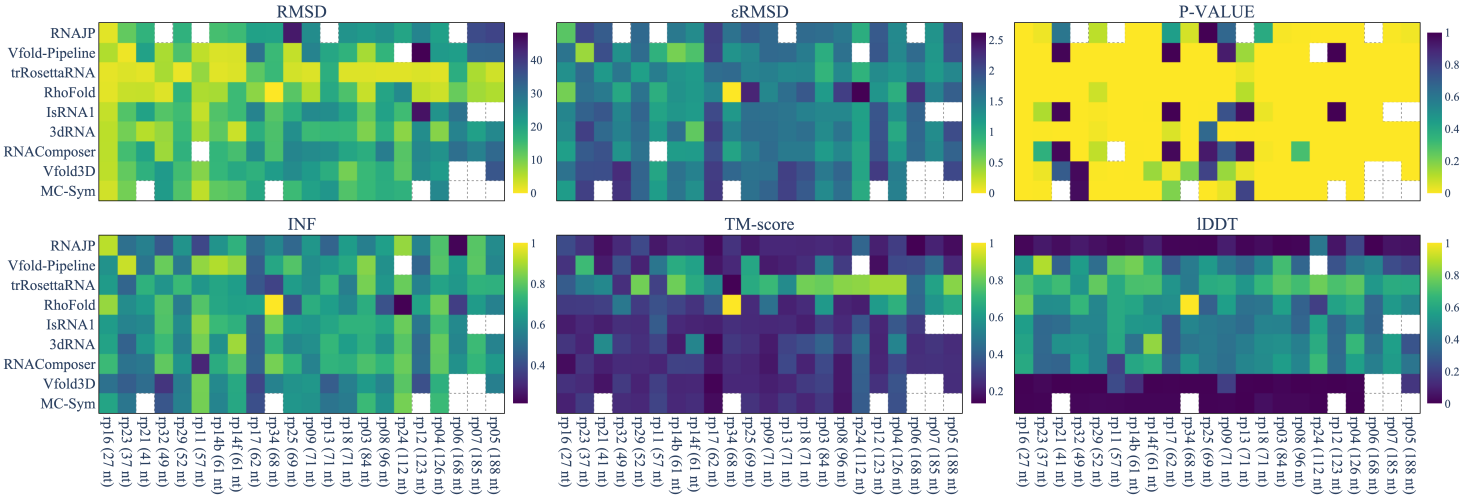

Figure 3. Results of a benchmark on RNA-Puzzles for each model described for each RNA. Missing values are due to a failure in predictions by the models or in the metric computation. Challenges are sorted by RNA sequence length. RNA length is provided in brackets. The best results are shown in yellow, while bad results are in dark.

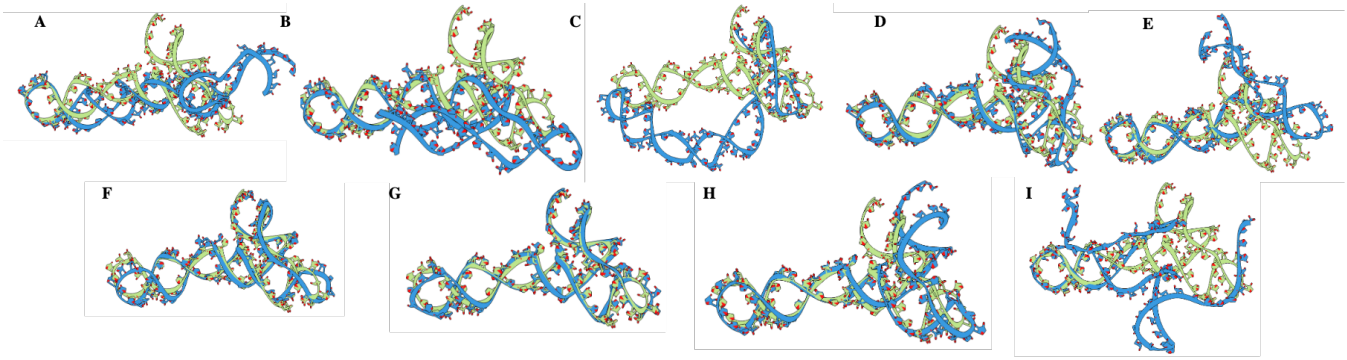

Figure 4. Predicting structures (blue) for RNAPuzzle 03 (rp03) (id: 3OWZ, 84 nucleotides) compared to native structure (green). A: MC-Sym. B: Vfold3D. C: RNAComposer. D: 3dRNA. E: IsRNA1. F: RhoFold. G: trRosettaRNA. H: Vfold-Pipeline. I: RNAJP. Alignment was done using CHIMERA (88) and Needleman-Wunsh algorithm (89).

the prediction.

Models	Time (27 nt)	Time (188 nt)
MC-Sym	∼1 min	∼2 hours
Vfold3D	∼10 min	∼2 hours
RNAComposer	∼1 min	∼5 min
3dRNA	∼1 hour	∼2 hours
IsRNA1	∼40 min	∼15 hours
RhoFold	∼1 min	∼10 min
trRosettaRNA	∼1 min	∼2 hours
Vfold-Pipeline	∼10 min	∼2 hours
RNAJP	∼2 hours	∼8 hours

Table 2. Approximate time for computation of RNA-Puzzles structures. The minimum time is for an RNA of 27 nucleotides, while the maximum time is computed for an RNA of 188 nucleotides. The computation time is an approximation, as it was run on web servers and might be slowed down by other pending jobs. The time reported for RhoFold is with the relaxation (which is slower than the raw prediction).

Dashboard

We provide a dashboard (Figure 5) with different visualisations of the predicted structures for the nine benchmarked models. The dashboard is freely available on the EvryRNA platform: https://evryrna.ibisc.univ-evry.fr. The user can choose which RNA to compare the predictions from among the different challenges of RNA-Puzzles (77). We also included some of the predictions we made on the CASP-RNA (81). All the metrics are also included in the dashboard. The aim of this dashboard is to make quick visualisations of our benchmarks done on available tools.

Discussion

Ab initio methods are physic-based approaches that incorporate different levels of granularity in nucleotide representation. The coarse-grained approach is a trade-off between efficiency in the representation and accuracy in the prediction. The force field force and energy function are another critical challenge for *ab initio* approach. If well chosen, it could guide the sampling procedure to low-energy structures that correspond to near-native structures. Otherwise, it could prevent the simulation from finding the path to good predictions and be obstructed in non-native predictions. Another bottleneck is the sampling method. It should simulate the folding process while bringing structures to the lowest energy. Molecular dynamics algorithms usually have good sampling procedures but are time-expensive. Finally, the reconstruction of coarse-grained methods is crucial to determining RNA 3D structures. It helps convert the approximation used to reduce computation time to real-world structures. Further development of *ab initio* models could incorporate a coarse-grained approach with efficient sample procedure and well-chosen force-field. It must be associated with full-atom reconstruction methods, adapted and efficient.

Template-based methods try to map sequences to structural motifs before merging them into a whole structure, which is then refined. These methods are more efficient than the *ab initio* while still being limited. The success of these methods relies on constructing a representative database and is usually based on secondary structures. It is, therefore, limited to the accuracy and throughput of secondary structure prediction. Moreover, the database constructed relies on the quality of RNA 3D known structures. Many RNA families have not been found yet, and the generalization property of these methods may struggle from this lack of data. Improvement of template-based methods could be based on the addition of existing physics-based methods that can predict structures not already seen. It could alleviate the prediction of unseen structures. Refining the structure after assembling could also be improved to best include fragments.

The performances of deep learning approaches seem promising. By using available data and self-distillation procedures, they perform well on RNA-Puzzles dataset. It remains limited, and the next AlphaFold for RNA has not yet been found (91). Performances of deep learning methods rely on available solved structures from the PDB. It could, therefore, easily overfit as the models have many parameters. The limited number of data is the main bottleneck to reproducing AlphaFold to RNAs. Deep learning methods are also considered a black box lacking interpretability. Knowing the folding process would highly increase RNA understanding and is a step the community would appreciate. Furthermore, deep learning models usually rely on MSA, which may not be as efficient as protein alignment. The generalization properties are, thus, limited as a lot of RNA families still need to be found. The integration of physics into deep learning methods could help reduce the black box trap as well as prevent models from overfitting. Using sequence-only methods could prevent the MSA-based methods that prevent the generalization process.

All the previously discussed models still need to be improved with the possibility of outputting multiple structures corresponding to environment-dependent RNA molecules. Works remain to allow the prediction of long non-coding RNAs. The sequence length is still a bottleneck, where integration of all possible interactions increases the complexity and limits existing models. We advise limiting the use of MSA for deep learning methods as it would easily fail with the arrival of unseen RNA families.

Hybrid work is also a direction that is taken by the community with recent solutions (92, 93) proposed in CASP-RNA (81). These solutions are usually a mix of previous methods to take the best of each of them. These recent methods are not yet available to users, so we did not include them in this work.

There remain intrinsic RNA limitations that restrict RNA structure modelization. First, the shortage of high-resolution RNA 3D structures prevents good annotation of RNA structures. Indeed, the flexibility of RNA molecules avoids cryo-EM or X-ray methods to annotate with high-resolution structures. Second, RNA 3D structures are sensitive to the solution environment. Small molecules, ligands or ions could strongly disrupt RNA folding, rarely integrated into current

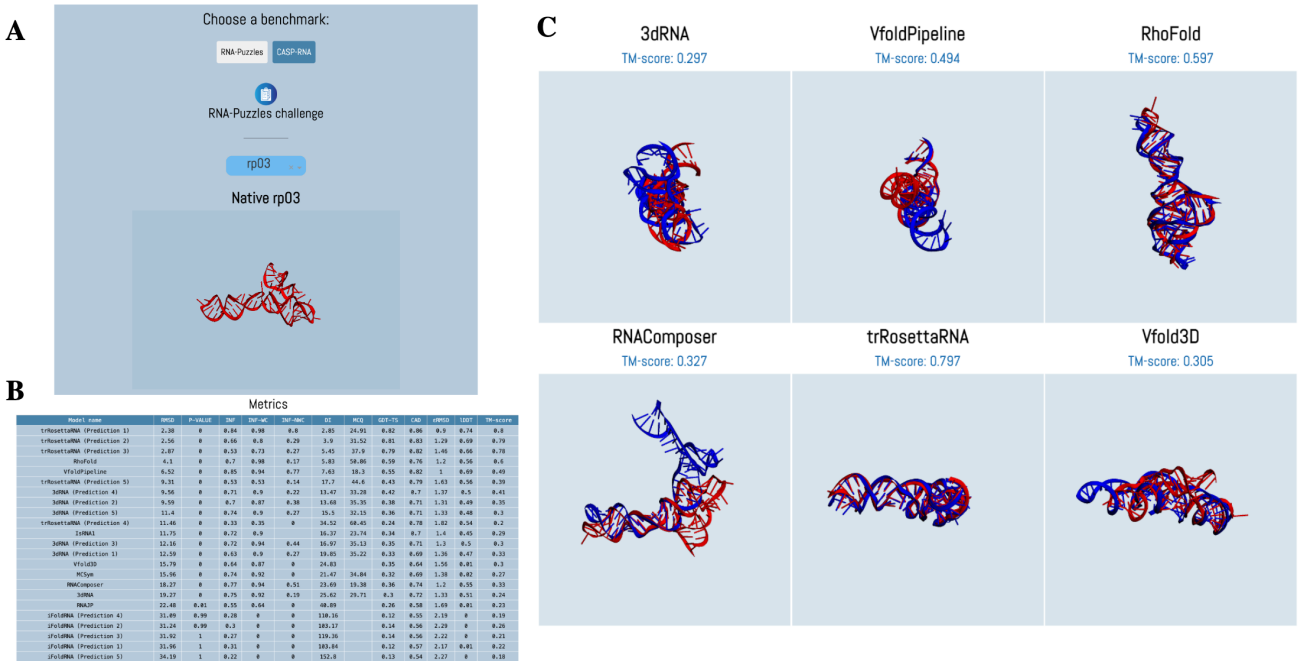

Model name	RMSD	P-VALUE	INF	INF-WC	INF-NWC	DI	MCQ	GDT-TS	CAD	clRMSD	lDDT	TM-score
trRosettaRNA (Prediction 1)	2.38	0	0.84	0.98	0.8	2.85	24.91	0.82	0.86	0.9	0.74	0.8
trRosettaRNA (Prediction 2)	2.56	0	0.66	0.8	0.29	3.9	31.52	0.81	0.83	1.29	0.69	0.79
trRosettaRNA (Prediction 3)	2.87	0	0.53	0.73	0.27	5.45	37.9	0.79	0.82	1.46	0.66	0.78
RhoFold	4.1	0	0.7	0.98	0.17	5.83	50.86	0.59	0.76	1.2	0.56	0.6
VfoldPipeline	6.52	0	0.85	0.94	0.77	7.63	18.3	0.55	0.82	1	0.69	0.49
trRosettaRNA (Prediction 5)	9.31	0	0.53	0.53	0.14	17.7	44.6	0.43	0.79	1.63	0.56	0.39
3dRNA (Prediction 4)	9.56	0	0.71	0.9	0.22	15.47	33.28	0.42	0.7	1.37	0.5	0.41
3dRNA (Prediction 2)	9.59	0	0.7	0.87	0.38	13.68	35.35	0.38	0.71	1.31	0.49	0.35
3dRNA (Prediction 5)	11.4	0	0.74	0.9	0.27	15.5	32.15	0.36	0.71	1.33	0.48	0.3
trRosettaRNA (Prediction 4)	11.46	0	0.33	0.35	0	34.52	60.45	0.24	0.78	1.82	0.54	0.2
IsRNA1	11.75	0	0.72	0.9		16.37	23.74	0.34	0.7	1.4	0.45	0.29
3dRNA (Prediction 3)	12.16	0	0.72	0.94	0.44	16.97	35.13	0.35	0.71	1.3	0.5	0.3
3dRNA (Prediction 1)	12.59	0	0.63	0.9	0.27	19.85	35.22	0.33	0.69	1.36	0.47	0.33
Vfold3D	15.79	0	0.64	0.87	0	24.83		0.35	0.64	1.56	0.41	0.3
MCSym	15.96	0	0.74	0.92	0	21.47	34.84	0.32	0.69	1.38	0.42	0.27
RNAComposer	18.27	0	0.77	0.94	0.51	23.69	19.38	0.36	0.74	1.2	0.55	0.33
3dRNA	19.27	0	0.75	0.92	0.19	25.62	29.71	0.3	0.72	1.33	0.51	0.24
RNA3P	22.48	0.01	0.55	0.64	0	40.09		0.26	0.58	1.69	0.01	0.23
iFoldRNA (Prediction 4)	31.09	0.99	0.28	0	0	110.16		0.12	0.55	2.19	0	0.19
iFoldRNA (Prediction 2)	31.24	0.99	0.3	0	0	103.17		0.14	0.56	2.29	0	0.20
iFoldRNA (Prediction 3)	31.92	1	0.27	0	0	119.36		0.14	0.56	2.22	0	0.21
iFoldRNA (Prediction 1)	31.96	1	0.31	0	0	103.64		0.12	0.57	2.17	0.01	0.22
iFoldRNA (Prediction 5)	34.19	1	0.22	0	0	152.8		0.13	0.54	2.27	0	0.18

Figure 5. Screenshot of the dashboard provided with the different predictions with native structure. A: The user can choose the RNA-Puzzles challenge to see the predictions. We also included some of the predictions for CASP-RNA (81). B: All the different metrics computed with RNAdvisor (78) for the given challenge. C: 3D visualisations of the different predictions of the benchmarked models. The native structure is coloured in red, while the predictions are in blue. The predictions are superimposed using the US-align (90) tool. The TM-score (84) of alignment is provided for each structure. Nine models are available in the dashboard.

state-of-the-art solutions. Third, no unique folding exists for a given RNA. RNA molecules are not static, and a given sequence can have many different structures of equivalent validity. Methods should be able to either integrate ions or ligands binding or explicitly predict multiple structures.

Future work should be done to increase the RNA-Puzzles dataset to understand model limitations best. Methods should also integrate environment properties like ions to best reproduce in vivo conditions. Individual work should be done to make model accessibility easy for community work. Web servers are standard but are also limited to automation.

ACKNOWLEDGEMENTS

This work is supported in part by UDOPIA-ANR-20-THIA-0013 and performed using HPC resources from GENCI/IDRIS (grant AD011014250). It was also partially supported by Labex DigiCosme (project ANR11LABEX0045DIGICOSME), operated by ANR as part of the program "Investissement d'Avenir" Idex ParisSaclay (ANR11IDEX000302).

Bibliography

1. Yuhua Zhu, Ling Zhu, Xinhua Wang, et al. Rna-based therapeutics: An overview and prospectus. *Cell Death & Disease*, 13:644, 2022. doi: 10.1038/s41419-022-05075-2.
2. Kailong Zhang, Shuai Li, Kristina Kappel, et al. Cryo-em structure of a 40 kda sam-iv riboswitch RNA at 3.7 Å resolution. *Nature Communications*, 10:5511, 2019. doi: 10.1038/s41467-019-13494-7.
3. D. Qin. Next-generation sequencing and its clinical application. *Cancer Biology and Medicine*, 16(1):4–10, 2019. doi: 10.20892/j.issn.2095-3941.2018.0055.
4. Helen M. Berman, John Westbrook, Zukang Feng, Gary Gilliland, T. N. Bhat, Helge Weissig, Ilya N. Shindyalov, and Philip E. Bourne. The Protein Data Bank. *Nucleic Acids Research*, 28(1):235–242, 01 2000. ISSN 0305-1048. doi: 10.1093/nar/28.1.235.
5. Ioanna Kalvari, Eric P. Nawrocki, Nancy Ontiveros-Palacios, Justyna Argasinska, Kevin Lamkiewicz, Manja Marz, Sam Griffiths-Jones, Claire Toffano-Nioche, Daniel Gautheret, Zasha Weinberg, Elena Rivas, Sean R. Eddy, Robert D. Finn, Alex Bateman, and Anton I. Petrov. Rfam 14: Expanded coverage of metagenomic, viral and microrna families. *Nucleic Acids Research*, 2020. doi: 10.1093/nar/gkaa1047.
6. Andriy Kryshtafovych, Torsten Schwede, Maya Topf, Krzysztof Fidelis, and John Moult. Critical assessment of methods of protein structure prediction (CASP)-round XIII. *Proteins*, 87 (12):1011–1020, 2019. doi: 10.1002/prot.25823.
7. Andrew W. Senior, Richard Evans, John Jumper, James Kirkpatrick, Laurent Sifre, Tim Green, Chongli Qin, Augustin Žídek, Alexander W. R. Nelson, Alex Bridgland, Hugo Penedones, Stig Petersen, Karen Simonyan, Steve Crossan, Pushmeet Kohli, David T. Jones, David Silver, Koray Kavukcuoglu, and Demis Hassabis. Improved protein structure prediction using potentials from deep learning. *Nature*, 577:706–710, 1 2020. ISSN 0028-0836. doi: 10.1038/s41586-019-1923-7.
8. John Jumper, Richard Evans, Alexander Pritzel, Tim Green, Michael Figurnov, Olaf Ronneberger, Kathryn Tunyasuvunakool, Russ Bates, Augustin Žídek, Anna Potapenko, Alex Bridgland, Clemens Meyer, Simon A. A. Kohl, Andrew J. Ballard, Andrew Cowie, Bernardino Romera-Paredes, Stanislav Nikolov, Rishub Jain, Jonas Adler, Trevor Back, Stig Petersen, David Reiman, Ellen Clancy, Michal Zielinski, Martin Steinegger, Michalina Pacholska, Tamas Berghammer, Sebastian Bodenstein, David Silver, Oriol Vinyals, Andrew W. Senior, Koray Kavukcuoglu, Pushmeet Kohli, and Demis Hassabis. Highly accurate protein structure prediction with AlphaFold. *Nature*, 596:583–589, 8 2021. ISSN 0028-0836. doi: 10.1038/s41586-021-03819-2.
9. Almudena Ponce-Salvatierra, Astha, Katarzyna Merdas, Chandran Nithin, Pritha Ghosh, Sunandan Mukherjee, and Janusz M. Bujnicki. Computational modeling of rna 3d structure based on experimental data. *Bioscience Reports*, 39, 2 2019. ISSN 0144-8463. doi: 10.1042/BSR20180430.
10. Bing Li, Yang Cao, Eric Westhof, and Zhichao Miao. Advances in rna 3d structure modeling using experimental data. *Frontiers in genetics*, 11:574485, 2020. ISSN 1664-8021. doi: 10.3389/fgene.2020.574485.
11. Jun Li and Shi-Jie Chen. Rna 3d structure prediction using coarse-grained models. *Frontiers in Molecular Biosciences*, 8, 7 2021. ISSN 2296-889X. doi: 10.3389/fmolb.2021.720937.
12. Xiujuan Ou, Yi Zhang, Yiduo Xiong, and Yi Xiao. Advances in rna 3d structure prediction. *Journal of Chemical Information and Modeling*, 62:5862–5874, 12 2022. ISSN 1549-9596. doi: 10.1021/acs.jcim.2c00939.
13. Fei Liu and Zhong-can Ou-Yang. Monte carlo simulation for single rna unfolding by force. *Biophysical Journal*, 88(1):76–84, 2005. ISSN 0006-3495. doi: 10.1529/biophysj.104.049239.
14. Xiao-Wei Qiang, Chen Zhang, Hai-Long Dong, Fu-Jia Tian, Hang Fu, Ya-Jun Yang, Liang Dai, Xing-Hua Zhang, and Zhi-Jie Tan. Multivalent cations reverse the twist-stretch coupling of rna. *Phys. Rev. Lett.*, 128:108103, Mar 2022. doi: 10.1103/PhysRevLett.128.108103.
15. Magdalena A. Jonikas, Randall J. Radmer, Alain Laederach, Rhiju Das, Samuel Pearlman, Daniel Herschlag, and Russ B. Altman. Coarse-grained modeling of large RNA molecules with knowledge-based potentials and structural filters. *RNA*, 15:189–199, 2 2009. ISSN 1355-8382. doi: 10.1261/rna.1270809.
16. Shantanu Sharma, Feng Ding, and Nikolay V. Dokholyan. iFoldRNA: three-dimensional RNA structure prediction and folding. *Bioinformatics*, 24:1951–1952, 9 2008. ISSN 1460-2059. doi: 10.1093/bioinformatics/btn328.
17. Petr Šulc, Flavio Romano, Thomas E. Ouldridge, Jonathan P. K. Doye, and Ard A. Louis. A nucleotide-level coarse-grained model of RNA. *J. Chem. Phys.*, 140:235102, 2014. doi: 10.1063/1.4881424.
18. Tristan Cragnolini, Yoann Laurin, Philippe Derreumaux, and Samuela Pasquali. Coarse-Grained HiRE-RNA Model for ab Initio RNA Folding beyond Simple Molecules, Including Noncanonical and Multiple Base Pairings. *Journal of Chemical Theory and Computation*, 11(7):3510–3522, 2015. doi: 10.1021/acs.jctc.5b00200. PMID: 26575783.
19. Michal J. Boniecki, Grzegorz Lach, Wayne K. Dawson, Konrad Tomala, Pawel Lukasz,

Tomasz Soltysinski, Kristian M. Rother, and Janusz M. Bujnicki. SimRNA: a coarse-grained method for RNA folding simulations and 3D structure prediction. *Nucleic Acids Research*, 44:e63–e63, 4 2016. ISSN 0305-1048. doi: 10.1093/nar/gkv1479.

20. Dong Zhang, Jun Li, and Shi-Jie Chen. IsRNA1: De Novo Prediction and Blind Screening of RNA 3D Structures. *Journal of Chemical Theory and Computation*, 17:1842–1857, 3 2021. ISSN 1549-9618. doi: 10.1021/acs.jctc.0c01148.
21. Dong Zhang, Shi jie Chen, and Ruhong Zhou. Modeling Noncanonical RNA Base Pairs by a Coarse-Grained IsRNA2 Model. *The journal of physical chemistry. B*, 2021.
22. Jun Li and Shi-Jie Chen. Rnajp: enhanced rna 3d structure predictions with non-canonical interactions and global topology sampling. *Nucleic Acids Research*, 51:3341–3356, 4 2023. ISSN 0305-1048. doi: 10.1093/nar/gkad122.
23. Peter Kerpedjiev, Christian H. Zu Siederdissen, and Ivo L. Hofacker. Predicting RNA 3d structure using a coarse-grain helix-centered model. *RNA*, 21:1110–1121, 2015. doi: 10.1261/rna.047522.114.
24. Jes Frellsen, Ida Moltke, Martin Thiim, Kanti V. Mardia, Jesper Ferkinghoff-Borg, and Thomas Hamelryck. A Probabilistic Model of RNA Conformational Space. *PLoS Computational Biology*, 5:e1000406, 6 2009. ISSN 1553-7358. doi: 10.1371/journal.pcbi.1000406.
25. Andrey Krokhotin, Kevin Houlihan, and Nikolay V. Dokholyan. iFoldRNA v2: folding RNA with constraints. *Bioinformatics*, 31:2891–2893, 9 2015. ISSN 1367-4803. doi: 10.1093/bioinformatics/btv221.
26. G.M. Torrie and J.P. Valleau. Nonphysical sampling distributions in monte carlo free-energy estimation: Umbrella sampling. *Journal of Computational Physics*, 23(2):187–199, 1977. ISSN 0021-9991. doi: https://doi.org/10.1016/0021-9991(77)90121-8.
27. Nicholas Metropolis, Arianna W. Rosenbluth, Marshall N. Rosenbluth, Augusta H. Teller, and Edward Teller. Equation of State Calculations by Fast Computing Machines. *The Journal of Chemical Physics*, 21(6):1087–1092, 12 2004. ISSN 0021-9606. doi: 10.1063/1.1699114.
28. Dong Zhang and Shi-Jie Chen. Isrna: An iterative simulated reference state approach to modeling correlated interactions in rna folding. *Journal of Chemical Theory and Computation*, 14(4):2230–2239, 2018. doi: 10.1021/acs.jctc.7b01228. PMID: 29499114.
29. Samuel C Flores, Yaqi Wan, Rick Russell, and Russ B Altman. Predicting RNA structure by multiple template homology modeling. *Pacific Symposium on Biocomputing. Pacific Symposium on Biocomputing*, page 216—227, 2010. ISSN 2335-6928. doi: 10.1142/9789814295291_0024.
30. Magdalena Rother, Kristian Rother, Tomasz Puton, and Janusz M. Bujnicki. ModeRNA: a tool for comparative modeling of RNA 3D structure. *Nucleic Acids Research*, 39:4007–4022, 5 2011. ISSN 1362-4962. doi: 10.1093/nar/gkq1320.
31. Rhiju Das and David Baker. Automated de novo prediction of native-like RNA tertiary structures. *Proceedings of the National Academy of Sciences of the United States of America*, 104:14664–9, 10 2007. doi: 10.1073/pnas.0703836104.
32. Andrew Martin Watkins, Ramya Rangan, and Rhiju Das. FARFAR2: Improved De Novo Rosetta Prediction of Complex Global RNA Folds. *Structure*, 28:963–976.e6, 8 2020. ISSN 09692126. doi: 10.1016/j.str.2020.05.011.
33. Marc Parisien and François Major. The MC-Fold and MC-Sym pipeline infers RNA structure from sequence data. *Nature*, 452:51–55, 3 2008. ISSN 0028-0836. doi: 10.1038/nature06684.
34. Mariusz Popenda, Marta Szachniuk, Maciej Antczak, Katarzyna J. Purzycka, Piotr Lukasiak, Natalia Bartol, Jacek Blazewicz, and Ryszard W. Adamiak. Automated 3D structure composition for large RNAs. *Nucleic Acids Research*, 40:e112–e112, 8 2012. ISSN 1362-4962. doi: 10.1093/nar/gks339.
35. C. Zhao, X. Xu, and S. J. Chen. Predicting rna structure with vfold. *Methods Mol Biol*, 1654: 3–15, 2017. doi: 10.1007/978-1-4939-7231-9_1.
36. Xiaojun Xu and Shi-Jie Chen. Hierarchical assembly of rna three-dimensional structures based on loop templates. *Journal of Physical Chemistry B*, 122:5327–5335, 2017. doi: 10.1021/acs.jpcb.7b01933.
37. Yi Zhang, Jun Wang, and Yi Xiao. 3drna: 3d structure prediction from linear to circular rnas. *Journal of Molecular Biology*, 434(11):167452, 2022. ISSN 0022-2836. doi: https://doi.org/10.1016/j.jmb.2022.167452. Computation Resources for Molecular Biology.
38. Jiajie Li, Shanshan Zhang, Dan Zhang, and Shi-Jie Chen. Vfold-pipeline: a web server for rna 3d structure prediction from sequences. *Bioinformatics*, 38(16):4042–4043, 2022. doi: 10.1093/bioinformatics/btab292.
39. Li Zhou, Xunxun Wang, Shixiong Yu, Ya-Lan Tan, and Zhi-Jie Tan. FebRNA: an automated fragment-ensemble-based model for building RNA 3D structures. *Biophysical Journal*, 121: 3381–3392, 2022.
40. Frank DiMaio, Michael D. Tyka, Matthew L. Baker, Wah Chiu, and David Baker. Refinement of protein structures into low-resolution density maps using rosetta. *Journal of Molecular Biology*, 392(1):181–190, 2009. doi: 10.1016/j.jmb.2009.07.008.
41. Song Cao and Shi-Jie Chen. Physics-based de novo prediction of rna 3d structures. *Journal of Physical Chemistry B*, 115:4216–4226, 2011. doi: 10.1021/jp110370s.
42. S. J. Weiner, P. A. Kollman, U. C. Singh, D. A. Case, C. Ghio, G. Alagona, S. Profeta, and P. Weiner. A new force field for molecular mechanical simulation of nucleic acids and proteins. *Journal of the American Chemical Society*, 106:765–784, 1984. doi: 10.1021/ja00315a051.
43. Alberto Perez, Iván Marchán, Daniel Svozil, Jiří Sponer, III Cheatham, Thomas E., Charles A. Laughton, and Modesto Orozco. Refinement of the amber force field for nucleic acids: Improving the description of α/γ conformers. *Biophysical Journal*, 92:3817–3829, 2007. doi: 10.1529/biophysj.106.097782.
44. W. Kabsch. A solution for the best rotation to relate two sets of vectors. *Acta Crystallographica Section A*, 32(5):922–923, 1976. doi: https://doi.org/10.1107/S0567739476001873.
45. Peter Güntert, Christian Mumenthaler, and Kurt Wüthrich. Torsion angle dynamics for nmr structure calculation with the new program dyana. *Journal of Molecular Biology*, 273(1): 283–298, October 1997. doi: 10.1006/jmbi.1997.1284.
46. Charles D. Schwieters, John J. Kuszewski, Nico Tjandra, and G. Marius Clore. The xplor-nih nmr molecular structure determination package. *Journal of Magnetic Resonance*, 160: 65–73, 2003. doi: 10.1016/S1090-7807(02)00014-9.
47. Jun Wang, Jian Wang, Yanzhao Huang, and Yi Xiao. 3dRNA v2.0: An Updated Web Server for RNA 3D Structure Prediction. *International Journal of Molecular Sciences*, 20:4116, 8 2019. ISSN 1422-0067. doi: 10.3390/ijms20174116.
48. Jian Wang, Yunjie Zhao, Chunyan Zhu, and Yi Xiao. 3dRNAscore: a distance and torsion angle dependent evaluation function of 3D RNA structures. *Nucleic Acids Research*, 43: e63–e63, 5 2015. ISSN 1362-4962. doi: 10.1093/nar/gkv141.
49. Yan Zhang, Jinfeng Wang, and Yun Xiao. 3drna: 3d structure prediction from linear to circular rnas. *Journal of Molecular Biology*, 434:167452, 2022. doi: 10.1016/j.jmb.2021.167452.
50. Ya-Lan Tan, Xunxun Wang, Shixiong Yu, Bengong Zhang, and Zhi-Jie Tan. cgrnasp: coarse-grained statistical potentials with residue separation for rna structure evaluation. *NAR Genomics and Bioinformatics*, 5(1), 03 2023. ISSN 2631-9268. doi: 10.1093/nargab/lqad016. lqad016.
51. S. Y. Le, R. Nussinov, and J. V. Maizel. Tree graphs of rna secondary structures and their comparisons. *Comput Biomed Res*, 22(5):461–473, Oct 1989. doi: 10.1016/0010-4809(89)90039-6.
52. Laiyi Fu, Yingxin Cao, Jie Wu, Qinke Peng, Qing Nie, and Xiaohui Xie. UFold: Fast and accurate RNA secondary structure prediction with deep learning. *Nucleic Acids Research*, 50(3):e14, 2022. doi: 10.1093/nar/gkab1074.
53. Kenta Sato, Masaru Akiyama, and Yasubumi Sakakibara. Rna secondary structure prediction using deep learning with thermodynamic integration. *Nature Communications*, 12:941, 2021. doi: 10.1038/s41467-021-21194-4.
54. Raphael J. L. Townshend, Stephan Eismann, Andrew M. Watkins, Ramya Rangan, Maria Karelina, Rhiju Das, and Ron O. Dror. Geometric deep learning of RNA structure. *Science*, 373:1047–1051, 8 2021. ISSN 0036-8075. doi: 10.1126/science.abe5650.
55. Jun Li, Wei Zhu, Jun Wang, Wenfei Li, Sheng Gong, Jian Zhang, and Wei Wang. RNA3DCNN: Local and global quality assessments of RNA 3D structures using 3D deep convolutional neural networks. *PLOS Computational Biology*, 14(11):1–18, 11 2018. doi: 10.1371/journal.pcbi.1006514.
56. Jaswinder Singh, Kuldip Paliwal, Jaspreet Singh, and Yaoqi Zhou. RNA Backbone Torsion and Pseudotorsion Angle Prediction Using Dilated Convolutional Neural Networks. *Journal of Chemical Information and Modeling*, 61:2610–2622, 6 2021. ISSN 1549-9596. doi: 10.1021/acs.jcim.1c00153.
57. Robin Pearce, Gilbert S. Omenn, and Yang Zhang. De novo RNA tertiary structure prediction at atomic resolution using geometric potentials from deep learning. *bioRxiv*, May 2022. doi: 10.1101/2022.05.15.491755.
58. Tao Shen, Zhihang Hu, Zhangzhi Peng, Jiayang Chen, Peng Xiong, Liang Hong, Liangzhen Zheng, Yixuan Wang, Irwin King, Sheng Wang, et al. E2efold-3d: End-to-end deep learning method for accurate de novo rna 3d structure prediction. *arXiv preprint arXiv:2207.01586*, 2022.
59. Minkyung Baek, Ryan McHugh, Ivan Anishchenko, David Baker, and Frank DiMaio. Accurate prediction of nucleic acid and protein-nucleic acid complexes using rosettafoldna. *bioRxiv*, 2022. doi: 10.1101/2022.09.09.507333.
60. Yuki Kagaya, Zicong Zhang, Nabil Ibtehaz, Xiao Wang, Tsukasa Nakamura, David Huang, and Daisuke Kihara. Nufold: A novel tertiary rna structure prediction method using deep learning with flexible nucleobase center representation. *bioRxiv*, 2023. doi: 10.1101/2023.09.20.558715.
61. Ashish Vaswani, Noam Shazeer, Niki Parmar, Jakob Uszkoreit, Llion Jones, Aidan N. Gomez, Lukasz Kaiser, and Illia Polosukhin. Attention Is All You Need, 2017.
62. Congzhou M. Sha, Jian Wang, and Nikolay V. Dokholyan. Predicting 3d rna structure from solely the nucleotide sequence using euclidean distance neural networks. *Biophysical Journal*, 122(3, Supplement 1):444a, 2023. ISSN 0006-3495. doi: https://doi.org/10.1016/j.bpj.2022.11.2396.
63. Y. Li, C. Zhang, C. Feng, and et al. Integrating end-to-end learning with deep geometrical potentials for ab initio rna structure prediction. *Nature Communications*, 14:5745, 2023. doi: 10.1038/s41467-023-41303-9.
64. W. Wang, C. Feng, R. Han, and et al. trrosettarna: automated prediction of rna 3d structure with transformer network. *Nat Commun*, 14:7266, 2023. doi: 10.1038/s41467-023-42528-4.
65. Jacob Devlin, Ming-Wei Chang, Kenton Lee, and Kristina Toutanova. BERT: Pre-training of Deep Bidirectional Transformers for Language Understanding, 2019.
66. Padideh Danaee, Mason Rouches, Michelle Wiley, Dezhong Deng, Liang Huang, and David Hendrix. bpRNA: large-scale automated annotation and analysis of RNA secondary structure. *Nucleic Acids Research*, 46(11):5381–5394, 05 2018. ISSN 0305-1048. doi: 10.1093/nar/gky285.
67. Dong C Liu and Jorge Nocedal. On the limited memory BFGS method for large scale optimization. *Mathematical Programming*, 45:503–528, 1989. doi: 10.1007/BF01589116.
68. Jiayang Chen, Zhihang Hu, Siqi Sun, Qingxiong Tan, Yixuan Wang, Qinze Yu, Licheng Zong, Liang Hong, Jin Xiao, Tao Shen, Irwin King, and Yu Li. Interpretable rna foundation model from unannotated data for highly accurate rna structure and function predictions, 2022.
69. J. Yang et al. Improved protein structure prediction using predicted interresidue orientations. *Proceedings of the National Academy of Sciences*, 117:1496, 2020. doi: 10.1073/pnas.1914677117.
70. Zheng Du et al. The trrosetta server for fast and accurate protein structure prediction. *Nature Protocols*, 16:5634–5651, 2021. doi: 10.1038/s41596-021-00594-7.
71. Haibin Su et al. Improved protein structure prediction using a new multi-scale network and homologous templates. *Advanced Science (Weinheim, Germany)*, 8:e2102592, 2021. doi: 10.1002/advs.202102592.
72. Jagtar Singh, Jack Hanson, Kuldip Paliwal, and Yaoqi Zhou. Rna secondary structure prediction using an ensemble of two-dimensional deep neural networks and transfer learning. *Nature Communications*, 10:5407, 2019. doi: 10.1038/s41467-019-13395-2.
73. Michael Hoffmann and Frank Noé. Generating valid euclidean distance matrices. *arXiv*, 2019.
74. Kengo Sato, Yuki Kato, Michiaki Hamada, Tatsuya Akutsu, and Kiyoshi Asai. Ipknot: fast and accurate prediction of rna secondary structures with pseudoknots using integer programming. *Bioinformatics*, 27:i85–i93, 2011. doi: 10.1093/bioinformatics/btr242.
75. Zion Perry, Anna Marie Pyle, and Chengxin Zhang. Arena: Rapid and accurate reconstruction of full atomic rna structures from coarse-grained models. *Journal Name*, X(X):XX–XX,

2023. doi: X.XXXX/XXXXXX.

76. Peter Eastman et al. Openmm 7: rapid development of high-performance algorithms for molecular dynamics. *PLOS Computational Biology*, 13:e1005659, 2017. doi: 10.1371/journal.pcbi.1005659.
77. José Cruz, Marc-Frédérick Blanchet, Michal Boniecki, Janusz Bujnicki, Shi-Jie Chen, Song Cao, Rhiju Das, Feng Ding, Nikolay Dokholyan, Samuel Flores, Lili Huang, Christopher Lavender, Veronique Lisi, François Major, Katarzyna Mikolajczak, Dinshaw Patel, Anna Philips, Tomasz Puton, John Santalucia, and Eric Westhof. RNA-Puzzles: A CASP-like evaluation of RNA three-dimensional structure prediction. *RNA (New York, N.Y.)*, 18:610–25, 02 2012. doi: 10.1261/rna.031054.111.
78. Clement Bernard, Guillaume Postic, Sahar Ghannay, and Fariza Tahi. Rnadvisor: a comprehensive benchmarking tool for the measure and prediction of rna structural model quality. *bioRxiv*, page 567018, 11 2023. doi: 10.1101/2023.11.14.567018.
79. Marcin Magnus, Maciej Antczak, Tomasz Zok, Jakub Wiedemann, Piotr Lukasiak, Yang Cao, Janusz M. Bujnicki, Eric Westhof, Marta Szachniuk, and Zhichao Miao. Rna-puzzles toolkit: a computational resource of rna 3d structure benchmark datasets, structure manipulation, and evaluation tools. *Nucleic Acids Research*, 2019. doi: 10.1093/nar/gkz1108.
80. Kengo Sato, Manato Akiyama, and Yasubumi Sakakibara. Rna secondary structure prediction using deep learning with thermodynamic integration. *Nature Communications*, 12:941, 12 2021. ISSN 2041-1723. doi: 10.1038/s41467-021-21194-4.
81. R Das, RC Kretsch, AJ Simpkin, and et al. Assessment of three-dimensional rna structure prediction in casp15. *Proteins*, 91(12):1747–1770, 2023. doi: 10.1002/prot.26602.
82. Marc Parisien, José Cruz, Eric Westhof, and François Major. New metrics for comparing and assessing discrepancies between RNA 3D structures and models. *RNA (New York, N.Y.)*, 15:1875–85, 09 2009. doi: 10.1261/rna.1700409.
83. Sandro Bottaro, Francesco Di Palma, and Giovanni Bussi. The Role of Nucleobase Interactions in RNA Structure and Dynamics. *Nucleic acids research*, 42, 10 2014. doi: 10.1093/nar/gku972.
84. Yang Zhang and Jeffrey Skolnick. Scoring function for automated assessment of protein structure template quality. *Proteins,* 57(4):702—710, December 2004. ISSN 0887-3585. doi: 10.1002/prot.20264.
85. Sha Gong, Chengxin Zhang, and Yang Zhang. Rna-align: quick and accurate alignment of rna 3d structures based on size-independent tm-scorerna. *Bioinformatics*, 35:4459–4461, 11 2019. ISSN 1367-4803. doi: 10.1093/bioinformatics/btz282.
86. Valerio Mariani, Marco Biasini, Alessandro Barbato, and Torsten Schwede. lddt: a local superposition-free score for comparing protein structures and models using distance difference tests. *Bioinformatics (Oxford, England)*, 29(21):2722–2728, 2013. doi: 10.1093/bioinformatics/btt473.
87. Christine Hajdin, Feng Ding, Nikolay Dokholyan, and Kevin Weeks. On the significance of an RNA tertiary structure prediction. *RNA (New York, N.Y.)*, 16:1340–9, 07 2010. doi: 10.1261/rna.1837410.
88. Thomas D. Goddard, Conrad C. Huang, Elaine C. Meng, Eric F. Pettersen, Gregory S. Couch, John H. Morris, and Thomas E. Ferrin. Ucsf chimerax: Meeting modern challenges in visualization and analysis. *Protein Science*, 27(1):14–25, 2018. doi: https://doi.org/10.1002/pro.3235.
89. Saul B. Needleman and Christian D. Wunsch. A general method applicable to the search for similarities in the amino acid sequence of two proteins. *Journal of Molecular Biology*, 48: 443–453, 3 1970. ISSN 00222836. doi: 10.1016/0022-2836(70)90057-4.
90. Chengxin Zhang, Morgan Shine, Anna Marie Pyle, and Yang Zhang. Us-align: Universal structure alignment of proteins, nucleic acids and macromolecular complexes. *Nature Methods*, 19:1109–1115, 2022.
91. Bohdan Schneider, Blake Alexander Sweeney, Alex Bateman, Jiri Cerny, Tomasz Zok, and Marta Szachniuk. When will RNA get its AlphaFold moment? *Nucleic Acids Research*, page gkad726, 09 2023. ISSN 0305-1048. doi: 10.1093/nar/gkad726.
92. Jun Li, Sicheng Zhang, and Shi-Jie Chen. Advancing rna 3d structure prediction: Exploring hierarchical and hybrid approaches in casp15. *Proteins: Structure, Function, and Bioinformatics*, n/a(n/a). doi: https://doi.org/10.1002/prot.26583.
93. Jun Li, Sicheng Zhang, and Shi-Jie Chen. Advancing rna 3d structure prediction: Exploring hierarchical and hybrid approaches in casp15. *Proteins: Structure, Function, and Bioinformatics*, 91(12):1779–1789, 2023. doi: https://doi.org/10.1002/prot.26583.